

Enhancing Energy Efficiency for Reconfigurable Intelligent Surfaces with Practical Power Models

Zhiyi Li, Jida Zhang, Jieao Zhu, Shi Jin, and Linglong Dai

Abstract—Reconfigurable intelligent surfaces (RISs) are widely considered a promising technology for future wireless communication systems. As an important indicator of RIS-assisted communication systems in green wireless communications, energy efficiency (EE) has recently received intensive research interest as an optimization target. However, most previous works have ignored the different power consumption between ON and OFF states of the PIN diodes attached to each RIS element. This oversight results in extensive unnecessary power consumption and reduction of actual EE due to the inaccurate power model. To address this issue, in this paper, we first utilize a practical power model for a RIS-assisted multi-user multiple-input single-output (MU-MISO) communication system, which takes into account the difference in power dissipation caused by ON-OFF states of RIS's PIN diodes. Based on this model, we formulate a more accurate EE optimization problem. However, this problem is non-convex and has mixed-integer properties, which poses a challenge for optimization. To solve the problem, an effective alternating optimization (AO) algorithm framework is utilized to optimize the base station and RIS beamforming precoder separately. To obtain the essential RIS beamforming precoder, we develop two effective methods based on maximum gradient search and SDP relaxation respectively. Theoretical analysis shows the exponential complexity of the original problem has been reduced to polynomial complexity. Simulation results demonstrate that the proposed algorithm outperforms the existing ones, leading to a significant increase in EE across a diverse set of scenarios.

Index Terms—Reconfigurable intelligent surface (RIS), energy efficiency (EE), non-convex mixed-integer programming, semi-definite programming (SDP).

I. INTRODUCTION

Recently, a new concept called reconfigurable intelligent surface (RIS) has attracted enormous attention and academic interest in wireless communications society. Specifically, RIS is a large reflection array composed of numerous nearly passive elements. By controllably tuning the phase-shifts of the incident signals, these elements are capable of cooperatively reflecting the signals towards desired directions with high

beamforming gain [2]–[4]. Due to its unique characteristics, RIS is expected to provide various performance improvements in wireless communications, including overcoming blockages, enhancing spectrum efficiency, and reducing energy consumption [5]–[7]. Among these, the reduction of energy consumption in RIS-assisted communication systems has been gaining increasing research interest, especially considering the growing demands for low-power massive connections and green radio in future wireless communications [8].

To realize energy-efficient RIS-aided communications, it is of practical importance to study the power consumption of RIS's hardware. Usually, RISs are manufactured with massive number of nearly passive elements, such as PIN diodes [9], [10], varactors [11], electrically controlled microelectromechanical systems (MEMS), and liquid crystals [12], which makes RIS-assisted systems energy-efficient. Among these hardware choices, PIN diodes have become the most prevailing tunable components, and have been widely applied to RISs due to their ability to serve as high-speed microwave switches with low insertion loss and low control voltage [13]. It is worth noting that, previous studies have pointed out the importance of considering the *dynamic power consumption* while constructing the power model for PIN diodes [14]. Specifically, each PIN diode consumes a typical power of around 10 mW when it is ON, and the power consumption varies based on its configuration [14]–[16]. For an RIS equipped with 512 elements, by assuming half of the PIN diodes are ON, the power dissipation will be 2.56 W. Compared to less than 10 W for base station (BS) transmit power and 10 mW for each user [17], the power dissipation of PIN diodes accounts for a significant proportion of the total power consumption in RIS-assisted communication systems. Therefore, when optimizing RIS configurations to meet energy-saving requirements in RIS-assisted systems, accurately modeling the power consumption attributed to PIN diodes is a crucial prerequisite.

A. Prior Works

Traditional communication performance indicator is the *spectral efficiency* (SE). The SE optimization of RIS-assisted systems has been extensively studied, and various optimization schemes have been proposed [18], [19]. To further reduce power consumption of RIS-assisted systems, a comprehensive performance indicator called the *energy efficiency* (EE) has been studied in the literature [20], [21]. The EE is defined as the ratio of SE to total power consumption. Thus, different from SE optimization, EE optimization is generally more complicated due to the additional fractional structure. Therefore,

This work was supported in part by the National Key Research and Development Program of China (Grant No.2020YFB1807201), in part by the National Natural Science Foundation of China (Grant No. 62031019), and in part by the European Commission through the H2020-MSCA-ITN META WIRELESS Research Project (Grant No. 956256). An earlier version of this paper was presented in part at the IEEE International Wireless Communications and Mobile Computing Conference (IEEE IWCMC'23), Marrakech, Morocco, June 2023 [1]. (*Corresponding author: Linglong Dai.*)

Z. Li, J. Zhang, J. Zhu, and L. Dai are with the Department of Electronic Engineering, Tsinghua University, Beijing 100084, China as well as the Beijing National Research Center for Information Science and Technology, Beijing, China (BNRist) (e-mails: {lizhiyi20, zhang-jd20, zja21}@mails.tsinghua.edu.cn, daill@tsinghua.edu.cn).

S. Jin is with the National Mobile Communications Research Laboratory, Southeast University, Nanjing 210096, China (e-mail: jinshi@seu.edu.cn).

SE optimization algorithms cannot be directly applied to EE optimization problems. To address the fractional structure that appears in the objective function of EE, effective algorithms such as sequential fractional programming (SFP) method [17] and quadratic transformation method [22] have been proposed.

However, the power consumption model used in EE optimization in previous works is highly inaccurate. Most of the existing EE optimization algorithms assume the RIS power dissipation to be constant, i.e., independent of RIS configurations [17], [22]. As mentioned earlier, for real-world phase-tuning components, the power caused by PIN diodes occupies a considerable portion of the total power consumption in RIS-assisted communication systems. Furthermore, the power consumption of PIN diodes in RIS varies significantly when they are configured to different states. Specifically, when configured to the ON state, i.e., the equivalent microwave switches admit the microwave signals, the diodes become extremely more power-hungry than in the OFF states [14], [16]. Consequently, although the power consumption model employed in prior studies simplifies the algorithm design, it introduces severe inaccuracy for actual PIN diode-controlled RIS elements, leading to high additional power consumption when designing algorithms to optimize EE. This issue becomes more pronounced in scenarios involving a large number of RIS elements [23], for instance, 1100 [24] and 2304 elements [10].

Thus, if we fail to consider the impact of the ON-OFF power difference, it can result in a significant increase in power consumption and a substantial reduction in EE, especially when the number of RIS elements increases. In order to acquire a high EE, an effective design of the ON-OFF states of RIS elements is required to achieve high beamforming gain with fewer ON-state elements. Prior to designing algorithms for optimal EE, it is necessary to introduce an actual model of RIS power consumption with the consideration of the ON-OFF power difference. Unfortunately, existing works mentioned above have neglected this crucial point, leading to a severe deviation from realistic scenarios. Therefore, *how to accurately model the RIS power consumption and design its configuration* is a critical aspect of achieving optimal EE in RIS-assisted communication systems.

B. Our Works

In this paper, we employ a more realistic power model for RIS-assisted systems, based on which we propose an effective algorithm to obtain optimal EE¹. Specifically, the contributions of this paper are summarized as follows:

- First, we introduce a realistic power dissipation model for downlink 1-bit RIS-assisted multi-user multiple-input single-output (MU-MISO) communication systems, which models the ON-OFF power difference of each RIS element. The proposed model better fits the actual RIS-assisted communication systems. Based on this model, we re-formulate the EE optimization problem.
- Next, to solve the formulated EE optimization problem, we adopt an alternating optimization (AO) algorithm

framework to optimize the BS and RIS precoder separately. However, obtaining the RIS precoder is NP-hard due to the non-convex mixed-integer property. To solve this problem, we apply two different methods based on maximum gradient search and SDP relaxation, respectively. The former method has lower computational complexity, while the latter one achieves better performance.

- Finally, we analyze the convergence and computational complexity of the proposed algorithms. Analysis results reveal that the exponential complexity of the original problem has been reduced to polynomial complexity. Simulation results verify the effectiveness of the proposed AO algorithmic framework with both methods, leading to a significant EE improvement in various scenarios.

C. Organization and Notation

Organization: The paper is structured as follows. In Section II, we establish the signal model and the definition of EE for downlink RIS-assisted MU-MISO systems, and then formulate the more accurate EE optimization problem with the consideration of RIS element ON-OFF power difference. In Section III, we introduce the AO algorithm framework to decouple the original problem into two subproblems, i.e., the power allocation problem, and the RIS analog beamforming problem. The analytical solution to the power allocation problem and the analysis of the computational complexity and convergence are also discussed. In Section IV, we focus on the non-convex mixed-integer RIS beamforming subproblem and provide two effective methods to acquire the near-optimal solution. The complexity and convergence analysis are also provided. In Section V, simulation results are provided to verify the performance and effectiveness of the proposed algorithm. Section VI concludes this paper.

Notation: \mathbb{R} and \mathbb{C} represent the sets of real and complex numbers, respectively. \mathbf{A}^* , \mathbf{A}^{-1} , \mathbf{A}^T , and \mathbf{A}^H indicate the conjugate, inverse, transpose, and conjugate transpose of matrix \mathbf{A} , respectively. $\mathcal{CN}(\mu, \sigma^2)$ refers to the complex univariate Gaussian distribution with mean μ and variance σ^2 . $\|\cdot\|_n$ denotes the \mathcal{L}_n -norm of its argument, respectively. $\text{diag}(\cdot)$ is the diagonal operation. $\mathbf{1}_{M \times N}$ and $\mathbf{0}_{M \times N}$ are $M \times N$ matrices with all elements equal to 1 and 0, respectively. $\text{tr}(\mathbf{X})$ refers to the trace of the matrix \mathbf{X} . $\mathbf{X} \succeq 0$ denotes a positive semi-definite matrix. \otimes , \odot denote the Kronecker and Hadamard product of two matrices respectively. \simeq indicates the equivalence of computational complexity order.

II. SYSTEM MODEL

In this section, we will first specify the signal model in Subsection II-A. Then, a more realistic power model and EE will be introduced in Subsection II-B with the consideration of ON-OFF power difference. Based on this, the EE optimization problem is formulated in Subsection II-C.

A. Signal Model

We consider a downlink RIS-assisted MU-MISO system, where K single-antenna users are served by an M -antenna BS.

¹Simulation codes will be provided to reproduce the results in this paper: <http://oa.ee.tsinghua.edu.cn/dailinglong/publications/publications.html>.

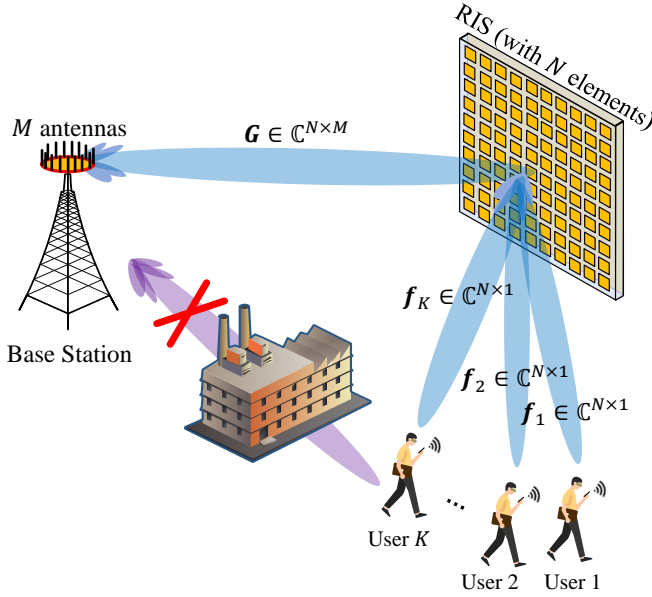


Fig. 1. RIS-assisted MU-MISO downlink system.

The direct BS-user link is assumed to be blocked as shown in Fig. 1. To ensure signal coverage and user experience, communication from BS to users is assisted by a RIS. The RIS comprises N_1 reflecting elements in the horizontal direction and N_2 reflecting elements in the vertical direction, resulting in a total of $N = N_1 \times N_2$ reflecting elements. Each RIS element is assumed to be binary-controlled, i.e., the diagonal phase-shift matrix Θ of the RIS only takes two possible values

$$\Theta = \text{diag}(e^{j\theta}) = \text{diag}([e^{j\theta_1}, e^{j\theta_2}, \dots, e^{j\theta_N}]), \theta_n \in \{0, \pi\}. \quad (1)$$

The RIS-BS channel is denoted as $\mathbf{G} \in \mathbb{C}^{N \times M}$, and the channel from RIS to the k -th user is denoted as $\mathbf{f}_k^H \in \mathbb{C}^{1 \times N}$. Then, the signal received by the users can be represented as

$$\mathbf{y} = \mathbf{F}^H \Theta \mathbf{G} \mathbf{W} \mathbf{s} + \mathbf{n}, \quad (2)$$

where $\mathbf{F} = [\mathbf{f}_1, \mathbf{f}_2, \dots, \mathbf{f}_K]$ represents the equivalent channel from RIS to each user, $\mathbf{s} = [s_1, s_2, \dots, s_K]^T$ represents the signal transmitted to each user, \mathbf{W} represents the digital precoding from BS with the power constraint $\text{tr}(\mathbf{W}^H \mathbf{W}) \leq P_{\max}$, and $\mathbf{n} \sim \mathcal{CN}(\mathbf{0}, \sigma_n^2 \mathbf{I}_K)$ represents the additive white Gaussian noise (AWGN) imposed at each receiver.

B. Energy Efficiency

The total power consumption can be modeled as follows

$$P_{\text{all}} = P_{\text{static}} + P_{\text{RIS}} + \nu^{-1} P_{\text{transmit}}, \quad (3)$$

in which P_{static} represents the overall static power consumption at BS, users, and RIS, $P_{\text{transmit}} = \text{tr}(\mathbf{W}^H \mathbf{W})$ represents the BS transmit power, and ν represents the efficiency of the power transmit amplifiers, which is considered as 1 in the following text. It is noteworthy that the power consumption of RIS elements is considered as a fixed value in most of the prior works [15], [17], [22], which is not in accord with the actual situation discussed in Section I. Thus, a binary-control

RIS is considered here, with the difference in ON-OFF power consumption of the PIN diode on each RIS element [14], i.e.,

$$P_{\text{RIS}} = \|\boldsymbol{\theta}\|_0 P_0, \theta_n \in \{0, \pi\}, \quad (4)$$

where P_0 is the power dissipation of each RIS element when the corresponding PIN diode is turned ON² by applying a bias current [9], and the n -th element θ_n of $\boldsymbol{\theta}$ is the phase-shift configuration of the n -th RIS element. With the discussions above, the SE and EE can be written as follows [25],

$$\text{SE}(\Theta, \mathbf{W}) = \sum_{k=1}^K \log_2 \left(1 + \frac{|\mathbf{f}_k^H \Theta \mathbf{G} \mathbf{w}_k|^2}{\sum_{k' \neq k} |\mathbf{f}_k^H \Theta \mathbf{G} \mathbf{w}_{k'}|^2 + \sigma_n^2} \right), \quad (5)$$

$$\text{EE}(\Theta, \mathbf{W}) = \frac{\text{BW} \times \text{SE}(\Theta, \mathbf{W})}{P_{\text{static}} + P_0 \|\boldsymbol{\theta}\|_0 + \text{tr}(\mathbf{W}^H \mathbf{W})}. \quad (6)$$

C. Problem Formulation

In this paper, our target is to acquire the maximum EE by jointly designing the digital beamforming matrix \mathbf{W} and the RIS analog beamforming vector $\boldsymbol{\theta}$, which can be expressed as

$$\mathcal{P}_0 : \max_{\Theta, \mathbf{W}} \text{EE}(\Theta, \mathbf{W}), \quad (7a)$$

$$\text{s.t. } \text{tr}(\mathbf{W}^H \mathbf{W}) \leq P_{\max}, \quad (7b)$$

$$\text{SE}_k \geq \text{SE}_{\min}, \forall k \in \mathcal{K}, \quad (7c)$$

$$\theta_n \in \{0, \pi\}, \forall n \in \mathcal{N}. \quad (7d)$$

As shown in (7c), we set a minimum spectrum efficiency value SE_{\min} for each user as a basic communication requirement.

The EE optimization problem \mathcal{P}_0 is a non-concave mixed integer programming due to the non-convex target function (7a) and the sparse constraint (7d), which makes the problem extremely difficult and complicated. In the next part of this paper, we will develop an effective optimization algorithm with an acceptable computational complexity.

III. ALGORITHMS

In this section, we will present an algorithm to address the EE optimization problem \mathcal{P}_0 . Firstly, we will introduce an alternating optimization procedure in order to acquire the optimal phase-shifts $\boldsymbol{\theta}$ and BS precoders \mathbf{W} in Subsection III-A. Then, the solution of the power allocation problem will be discussed in Subsection III-B, i.e. the optimal \mathbf{W} with fixed $\boldsymbol{\theta}$. The convergence and the computational complexity of the algorithm will be discussed in Subsection III-C. For clarity, the algorithm to solve the RIS analog beamforming problem will be designed in the next section, whose difficulty and complexity lead to a separate section to discuss.

A. Alternating Optimization

In order to fully eliminate the interference of signal in different channels, the Zero-Forcing (ZF) digital precoder [26] can be utilized here to obtain a feasible solution, i.e.,

$$\mathbf{W} = \mathbf{H} (\mathbf{H}^H \mathbf{H})^{-1} \mathbf{P}^{\frac{1}{2}}, \quad (8)$$

²In this paper, we assume that the reflection coefficient of each RIS element is tuned by only one PIN diode.

where $\mathbf{H}^H = \mathbf{F}^H \mathbf{\Theta} \mathbf{G}$ represents the cascade channel from BS to users, the diagonal matrix \mathbf{P} represents the power allocation of each user, whose k -th diagonal element p_k represents the signal power received by the k -th user. With the ZF precoder, the signal received by users can be rewritten as follows:

$$\mathbf{y} = \mathbf{P}^{\frac{1}{2}} \mathbf{s} + \mathbf{n}, \quad (9)$$

and the corresponding transmit power constraints (7b) of \mathcal{P}_0 can be rewritten as

$$\text{tr}(\mathbf{W}^H \mathbf{W}) = \text{tr}\left(\mathbf{P}^{\frac{1}{2}} (\mathbf{H}^H \mathbf{H})^{-1} \mathbf{P}^{\frac{1}{2}}\right) \leq P_{\max}. \quad (10)$$

Thus, the spectrum efficiency can also be rewritten as

$$\text{SE}(\mathbf{\Theta}, \mathbf{P}) = \text{SE}(\mathbf{P}) = \sum_{k=1}^K \log_2 \left(1 + \frac{p_k}{\sigma_n^2}\right), \quad (11)$$

where p_k represents the k -th diagonal element of \mathbf{P} , i.e. the received signal power of the k -th user. Then, the problem \mathcal{P}_0 can be expressed as

$$\mathcal{P}'_0 : \max_{\mathbf{\Theta}, \mathbf{P}} \frac{\text{BW} \sum_{k=1}^K \log_2 \left(1 + \frac{p_k}{\sigma_n^2}\right)}{P_{\text{static}} + P_0 \|\boldsymbol{\theta}\|_0 + \text{tr}\left(\mathbf{P}^{\frac{1}{2}} (\mathbf{H}^H \mathbf{H})^{-1} \mathbf{P}^{\frac{1}{2}}\right)}, \quad (12a)$$

$$\text{s.t. } \text{tr}\left(\mathbf{P}^{\frac{1}{2}} (\mathbf{H}^H \mathbf{H})^{-1} \mathbf{P}^{\frac{1}{2}}\right) \leq P_{\max}, \quad (12b)$$

$$p_k \geq p_{\min}, \quad \forall k \in \mathcal{K} \quad (12c)$$

$$\theta_n \in \{0, \pi\}, \quad \forall n \in \mathcal{N}, \quad (12d)$$

where $p_{\min} = \sigma^2 (2^{\text{SE}_{\min}} - 1)$ represents the minimum received power requirement of each user in order to ensure the basic communication spectrum efficiency SE_{\min} .

With the discussions above, the original optimization problem \mathcal{P}_0 is transformed to \mathcal{P}'_0 with the optimization variables $\mathbf{\Theta}$ and \mathbf{P} . Considering the difficulty to acquire optimal $\mathbf{\Theta}$ and \mathbf{P} simultaneously, an alternating optimization (AO) algorithm can be applied to solve the problem. Firstly, the power allocation matrix \mathbf{P} can be optimized with fixed $\mathbf{\Theta}$, and then the RIS analog beamforming matrix $\mathbf{\Theta}$ can be optimized with fixed \mathbf{P} . Thus, \mathbf{P} and $\mathbf{\Theta}$ can be updated until convergence.

B. Solution of the Power Allocation Problem

According to the AO algorithm of problem \mathcal{P}'_0 , the first step is to find the optimal power allocation matrix \mathbf{P} with the fixed RIS configuration $\mathbf{\Theta}$, which leads to a power allocation problem as follows:

$$\mathcal{P}_1 : \max_{\mathbf{P}} \frac{1}{P_1 + \sum_{k=1}^K p_k t_k} \sum_{k=1}^K \log \left(1 + \frac{p_k}{\sigma_n^2}\right), \quad (13a)$$

$$\text{s.t. } \sum_{k=1}^K p_k t_k \leq P_{\max}, \quad (13b)$$

$$p_k \geq p_{\min}, \quad (13c)$$

where $P_1 \triangleq P_{\text{static}} + P_0 \|\boldsymbol{\theta}\|_0$ and t_k is the k -th diagonal element of $(\mathbf{H}^H \mathbf{H})^{-1}$. Although the constraints (13b) and (13c) are both affine, the problem \mathcal{P}_1 is also a thorny matter due to the non-concave target function (13a). One feasible

method is to introduce a relaxation variable in order to convert fractions to polynomials. Thus, the problem above can be solved by Dinkelbach's method as follows [17]:

$$\mathbf{P}^{(i)} = \arg \max_{\mathbf{P}} \sum_{k=1}^K \log_2 \left(1 + \frac{p_k}{\sigma_n^2}\right) - \lambda^{(i-1)} \left(P_1 + \sum_{k=1}^K p_k t_k\right), \quad (14a)$$

$$\text{s.t. } \sum_{k=1}^K p_k t_k \leq P_{\max}, \quad p_k \geq p_{\min}$$

$$\lambda^{(i)} = \frac{1}{P_1 + \sum_{k=1}^K p_k^{(i)} t_k} \sum_{k=1}^K \log_2 \left(1 + \frac{p_k^{(i)}}{\sigma_n^2}\right). \quad (14b)$$

The optimization problem (14a) is convex, whose analytical solution will be given in **Appendix A**. Then, the procedures to solve \mathcal{P}_1 can be summarized in **Algorithm 1**.

Algorithm 1 Power Allocation Problem

Input: Numbers of users K ; Power fading coefficients t_1, \dots, t_K ; Variance of the AWGN σ_n^2 .

Output: Power allocation matrix $\mathbf{P} = \text{diag}(p_1, p_2, \dots, p_K)$.

- 1: Find ζ such that: $\sum_k \{\zeta - t_k \sigma_n^2, t_k p_{\min}\} = P_{\max}$
 - 2: **for** $i = 1, 2, \dots, N_{\text{iter}}$ **do**
 - 3: $\xi^{(i)} \leftarrow \min \{\zeta, 1 / (\lambda^{(i-1)} \log 2)\}$.
 - 4: $p_k^{(i)} \leftarrow \max \{(\xi - t_k \sigma_n^2) / t_k, p_{\min}\}$.
 - 5: $\lambda^{(i)} \leftarrow \sum_k \log_2 \left\{1 + p_k^{(i)} / \sigma_n^2\right\} / (P_1 + \sum_k p_k t_k)$.
 - 6: **end for**
 - 7: **return** Optimized \mathbf{P}
-

C. Complexity & Convergence Analysis

Firstly, the computational complexity will be derived as follows. According to **Algorithm 1**, the complexity of the power allocation problem mainly comes from the iteration step. For each step, the values of ξ , p_k , and λ are calculated in turn, which leads to a linear complexity $\mathcal{O}(K)$. Thus, the computational complexity of the power allocation problem is $\mathcal{O}(N_{\text{iter}} K)$, where N_{iter} represents the number of iterations of the algorithm. The computational complexity of the RIS beamforming problem will be discussed in Subsection IV-C.

We focus on the convergence of the power allocation problem. According to the optimality of $p_k^{(i)}$ in (14a), we have

$$\begin{aligned} \mathcal{P}(p_k^{(i)}) &= \sum_{k=1}^K \log_2 \left(1 + \frac{p_k^{(i)}}{\sigma_n^2}\right) - \lambda^{(i-1)} \left(P_1 + \sum_{k=1}^K p_k^{(i)} t_k\right) \\ &\geq \mathcal{P}(p_k^{(i-1)}) = \sum_{k=1}^K \log_2 \left(1 + \frac{p_k^{(i-1)}}{\sigma_n^2}\right) \\ &\quad - \lambda^{(i-1)} \left(P_1 + \sum_{k=1}^K p_k^{(i-1)} t_k\right) = 0. \end{aligned} \quad (15)$$

Therefore, it is obvious that $\lambda^{(i)} \geq \lambda^{(i-1)}$, which proves the convergence of \mathcal{P}_1 .

As for the convergence of AO algorithm, consider the j -th iteration where $\text{EE}_1^{(j)}$ denotes the EE after power allocation (optimizing \mathbf{P} with fixed Θ) and $\text{EE}_2^{(j)}$ denotes the EE after RIS beamforming (optimizing Θ with fixed \mathbf{P}). With the discussion about the convergence of \mathcal{P}_1 , it is ensured that $\text{EE}_1^{(j)} \geq \text{EE}_2^{(j-1)}$. As long as the RIS beamforming problem can be solved effectively, i.e. the algorithm of the problem satisfies $\text{EE}_2^{(j)} \geq \text{EE}_1^{(j)}$, which will be explained in detail in Section IV, we will have $\text{EE}_2^{(j)} \geq \text{EE}_1^{(j)} \geq \text{EE}_2^{(j-1)}$. This proves the convergence of the AO algorithm.

IV. RIS ANALOG BEAMFORMING

In this section, we focus on the discussion about the algorithm of RIS analog beamforming. According to the AO algorithm in Section III, the next step is to optimize Θ with fixed \mathbf{P} , which can be expressed as follows,

$$\mathcal{P}_2 : \min_{\Theta} P_0 \|\theta\|_0 + \sum_{k=1}^K p_k t_k, \quad (16a)$$

$$\text{s.t.} \quad \sum_{k=1}^K p_k t_k \leq P_{\max}, \quad (16b)$$

$$\theta_n \in \{0, \pi\}, \quad \forall n \in \mathcal{N}. \quad (16c)$$

We denote $\mathbf{q} = e^{j\theta}$. Since $\theta_n \in \{0, \pi\}$, we have $q_n \in \{-1, 1\}$ and $\|\theta\|_0 = -\frac{1}{2} \mathbf{1}^T \mathbf{q} + N/2$. Then \mathcal{P}_2 can be rewritten as

$$\mathcal{P}'_2 : \min_{\mathbf{q}} -\frac{1}{2} P_0 \mathbf{1}^T \mathbf{q} + \sum_{k=1}^K p_k t_k, \quad (17a)$$

$$\text{s.t.} \quad \sum_{k=1}^K p_k t_k \leq P_{\max}, \quad (17b)$$

$$q_n \in \{-1, 1\}, \quad \forall n \in \mathcal{N}. \quad (17c)$$

It should be noted that t_k is a function of \mathbf{q} in \mathcal{P}'_2 . As we have mentioned, the non-convexity of the target function (16a) and the discrete constraint (16c) makes \mathcal{P}_2 difficult to solve. Generally, it is an NP-hard problem due to the integer constraint (16c), so it is almost impossible to acquire an optimal solution with low computational time. However, some effective methods such as heuristic search and proper relaxations are helpful to obtain a computationally feasible solution. In Subsection IV-A we propose an algorithm based on maximum gradient search, which has a low computational cost and thus can solve the problem efficiently. Due to the fact that gradient-based algorithms may converge to local optimum in some situations, an alternative algorithm based on SDP relaxation is proposed in Subsection IV-B, and the appropriate solution of problem \mathcal{P}_2 will be given. The computational complexity and convergence will be analyzed in Subsection IV-C.

A. Search with the Maximum Gradient

One of the most popular solutions to mixed integer programming \mathcal{P}'_2 is based on searching methods, such as the Branch and Bound method. The fatal defect of this type of method

is that it usually has unacceptable computational complexity, e.g., $\mathcal{O}(2^N)$. Although gradient descent methods in continuous variable optimization cannot be applied to discrete cases directly, they still provide some insights. In discrete cases, the direction with the maximum gradient value can also be regarded as the fastest direction to make the objective function decline. Then, we can design the searching method with the maximum gradient.

Firstly, the gradient of the objective function in (17a) (defined as $g(\mathbf{q})$) can be expressed as

$$\begin{aligned} \frac{\partial g(\mathbf{q})}{\partial q_n} &= -\frac{1}{2} P_0 + \sum_{k=1}^K p_k \left[\frac{\partial (\mathbf{H}^H \mathbf{H})^{-1}}{\partial q_n} \right]_{(k,k)} \\ &= -\frac{1}{2} P_0 - \sum_{k=1}^K p_k \left[(\mathbf{H}^H \mathbf{H})^{-1} \frac{\partial \mathbf{H}^H \mathbf{H}}{\partial q_n} (\mathbf{H}^H \mathbf{H})^{-1} \right]_{(k,k)} \\ &= -\frac{1}{2} P_0 - \sum_{k=1}^K p_k \left[(\mathbf{H}^H \mathbf{H})^{-1} (\mathbf{F}^H \text{diag}(\mathbf{e}_n) \mathbf{G} \mathbf{H} \right. \\ &\quad \left. + \mathbf{H}^H \mathbf{G}^H \text{diag}(\mathbf{e}_n) \mathbf{F}) (\mathbf{H}^H \mathbf{H})^{-1} \right]_{(k,k)}. \end{aligned} \quad (18)$$

Based on (18), we can design the searching method. Then, each q_n changes from large $\partial g / \partial q_n \times q_n$ to small ones, during which the value of $g(\mathbf{q})$ and the feasibility of \mathbf{q} will be verified. If the updated \mathbf{q}^* is a feasible and better solution than \mathbf{q} , i.e. $g(\mathbf{q}^*) \leq g(\mathbf{q})$, the update will be kept and go on to the next. Details of the method are summarized in **Algorithm 2**.

Algorithm 2 Search with the Maximum Gradient

Input: Number of RIS elements N ; Channel matrix \mathbf{F}, \mathbf{G} ;

Energy consumption of each RIS element P_{RIS} ; Initial RIS state $\mathbf{q}^{(0)}$; Ratio of each epoch ρ ; Threshold ε .

Output: RIS beamforming state \mathbf{q} .

- 1: **while** $\|\mathbf{q}^{(i)} - \mathbf{q}^{(i-1)}\|_0 \geq \varepsilon$ **do**
 - 2: Calculate the gradient of $g(\mathbf{q}^{(i-1)})$ according to (18).
 - 3: Sort the product of \mathbf{q}_n and $\partial g(\mathbf{q}) / \partial q_n$ in descending order d .
 - 4: $\mathbf{q}^{(i)} \leftarrow \mathbf{q}^{(i-1)}$
 - 5: **for** $j = 1, 2, \dots, \text{round}(\rho N)$ **do**
 - 6: $\mathbf{q}_{d_j}^{(i)} \leftarrow -\mathbf{q}_{d_j}^{(i)}$
 - 7: **if** This solution $\mathbf{q}^{(i)}$ is unfeasible or more energy consumption **then**
 - 8: $\mathbf{q}_{d_j}^{(i)} \leftarrow -\mathbf{q}_{d_j}^{(i)}$
 - 9: **end if**
 - 10: **end for**
 - 11: $i \leftarrow i + 1$
 - 12: **end while**
 - 13: **return** \mathbf{q}
-

B. SDP Relaxation

In the previous subsection, the RIS phase-shift vector \mathbf{q} is obtained by applying an effective heuristic search to the problem \mathcal{P}'_2 in **Algorithm 2**, which does not guarantee the optimality. A more reasonable approach is to construct a solution to \mathcal{P}'_2 by analyzing the inherent mathematical structure of this optimization problem. Note that the constraints (17b) (or (16b)) are applied to the trace of the inverse matrix of $\mathbf{H}^H \mathbf{H}$, which is further a quadratic function of \mathbf{q} according to the definition of \mathbf{H} . Thus, if we replace \mathbf{q} by a quadratic variable $\mathbf{X} \in \mathbb{R}^{(N+1) \times (N+1)}$ defined as

$$\mathbf{X} = \begin{bmatrix} \mathbf{q}\mathbf{q}^T & \mathbf{q} \\ \mathbf{q}^T & 1 \end{bmatrix}, \quad (19)$$

then the constraint (17b) can be expressed as $\text{tr}(\mathbf{Y}^{-1})$, where the elements of \mathbf{Y} are linear combinations of the elements in \mathbf{X} . Since linear transform does not alter convexity, $\text{tr}(\mathbf{Y}^{-1})$ is a convex function of the new matrix argument \mathbf{X} . Through this change of variable, i.e., $\mathbf{q} \rightarrow \mathbf{X}$, the target function (17a) of \mathcal{P}'_2 is made convex simultaneously. Thus, \mathcal{P}'_2 can be rewritten as

$$\mathcal{P}_3 : \min_{\mathbf{X}} -\frac{1}{4} P_{\text{RIS}} \text{tr}(\mathbf{E}_0 \mathbf{X}) + \text{tr}(\mathbf{F}_0^H (\mathbf{X} \odot \mathbf{G}_0) \mathbf{F}_0 \mathbf{P}^{-1})^{-1}, \quad (20a)$$

$$\text{s.t. } \text{tr}((\mathbf{F}_0^H (\mathbf{X} \odot \mathbf{G}_0) \mathbf{F}_0 \mathbf{P}^{-1})^{-1}) \leq P_{\text{max}}, \quad (20b)$$

$$\text{tr}(\mathbf{E}_{i,i} \mathbf{X}) = 1, \quad i \in 1, 2, \dots, N+1, \quad (20c)$$

$$\mathbf{X} \succeq 0, \quad (20d)$$

$$\text{rank}(\mathbf{X}) = 1, \quad (20e)$$

where $\mathbf{E}_0 \in \mathbb{R}^{(N+1) \times (N+1)}$, $\mathbf{E}_{i,i} \in \mathbb{R}^{(N+1) \times (N+1)}$, $\mathbf{F}_0 \in \mathbb{C}^{(N+1) \times K}$, and $\mathbf{G}_0 \in \mathbb{R}^{(N+1) \times (N+1)}$ is defined as

$$\mathbf{E}_0 = \begin{bmatrix} \mathbf{0}_{N \times N} & \mathbf{1}_{N \times 1} \\ \mathbf{1}_{1 \times N} & 0 \end{bmatrix}, \mathbf{E}_{i,i} = \text{diag}(e_i), \quad (21)$$

$$\mathbf{G}_0 = \begin{bmatrix} \mathbf{G}\mathbf{G}^H & \mathbf{0}_{N \times 1} \\ \mathbf{0}_{1 \times N} & 0 \end{bmatrix}, \mathbf{F}_0 = \begin{bmatrix} \mathbf{F} \\ \mathbf{0}_{1 \times K} \end{bmatrix}.$$

The equivalence between \mathcal{P}'_2 and \mathcal{P}_3 is proved in **Appendix B**.

After the conversion of the optimization variables, the objective function (20a) and the constraints (20b), (20c), and (20d) are all convex. Therefore, the only challenge is the non-convexity of (20e). If we relax the constraint (20e), which is called SDR [18], [27], the optimization problem will be expressed as a convex SDP problem

$$\mathcal{P}'_3 : \min_{\mathbf{X}} -\frac{1}{4} P_{\text{RIS}} \text{tr}(\mathbf{E}_0 \mathbf{X}) + \text{tr}(\mathbf{F}_0^H (\mathbf{X} \odot \mathbf{G}_0) \mathbf{F}_0 \mathbf{P}^{-1})^{-1}, \quad (22a)$$

$$\text{s.t. } \text{tr}((\mathbf{F}_0^H (\mathbf{X} \odot \mathbf{G}_0) \mathbf{F}_0 \mathbf{P}^{-1})^{-1}) \leq P_{\text{max}}, \quad (22b)$$

$$\text{tr}(\mathbf{E}_{i,i} \mathbf{X}) = 1, \quad i \in 1, 2, \dots, N+1, \quad (22c)$$

$$\mathbf{X} \succeq 0. \quad (22d)$$

The problem \mathcal{P}'_3 is a standard convex semi-definite programming, which can be solved with general procedures like the interior-point method by CVX solvers [28].

The next step is to acquire the low-rank solution \mathbf{X} of

\mathcal{P}_3 (i.e. \mathbf{q} of \mathcal{P}'_2) from the solution $\tilde{\mathbf{X}}$ of \mathcal{P}'_3 . According to the positive definiteness of $\tilde{\mathbf{X}}$, we can define $\mathbf{V} = [\mathbf{v}_1, \mathbf{v}_2, \dots, \mathbf{v}_N] \in \mathbb{R}^{N \times N}$ as $\mathbf{V}^T \mathbf{V} = \tilde{\mathbf{X}}(1 : N, 1 : N)$. Randomly select $\mathbf{u} \in \mathbb{R}^N$ from uniform distribution on N -dimensional sphere (an implementation is to construct $\tilde{\mathbf{u}}$ where $\tilde{u}_i \sim \mathcal{N}(0, 1)$, then $\mathbf{u} = \tilde{\mathbf{u}} / \|\tilde{\mathbf{u}}\|$). Then, the estimation \tilde{q}_i is the sign of projection of \mathbf{v}_i to \mathbf{u} , i.e. $\tilde{q}_i = \text{sgn}(\mathbf{u}^T \mathbf{v}_i)$. We can repeat the procedure for times to select the optimal solution. The method based on SDP relaxation can be summarized in **Algorithm 3**.

Algorithm 3 SDP Relaxation

Input: Number of RIS elements N ; Channel matrix \mathbf{F}, \mathbf{G} ;
Energy consumption of each RIS element P_{RIS} .

Output: RIS beamforming state \mathbf{q} .

- 1: Calculate $\mathbf{F}_0, \mathbf{G}_0$.
 - 2: Solve the problem \mathcal{P}'_3 with the standard SDP procedures and acquire the optimal $\tilde{\mathbf{X}}$.
 - 3: $\mathbf{V} \leftarrow (\tilde{\mathbf{X}}(1 : N, 1 : N))^{\frac{1}{2}}$
 - 4: **for** $i = 1, 2, \dots, N_{\text{SDP}}$ **do**
 - 5: Randomly choose $\tilde{\mathbf{u}}^{(i)}$ with $\tilde{u}_n^{(i)} \sim \mathcal{N}(0, 1)$.
 - 6: $\mathbf{u}^{(i)} \leftarrow \tilde{\mathbf{u}}^{(i)} / \|\tilde{\mathbf{u}}^{(i)}\|$
 - 7: $\hat{q}_n^{(i)} \leftarrow \text{sgn}(\mathbf{v}_n^T \mathbf{u}^{(i)})$
 - 8: $g^{(i)} \leftarrow -\frac{1}{2} P_0 \mathbf{1}^T \mathbf{q}^{(i)} + \sum_{k=1}^K p_k t_k^{(i)}$
 - 9: **end for**
 - 10: Select the $\mathbf{q}^{(i)}$ as \mathbf{q} corresponding to the minimum $g^{(i)}$.
 - 11: **return** \mathbf{q}
-

C. Complexity & Convergence Analysis

The original RIS analog beamforming problem \mathcal{P}_2 or \mathcal{P}'_2 is NP-hard, which means the computational complexity for the optimal solution is at least $\mathcal{O}(2^N)$. This is an unacceptable thing, especially for the RIS with a large number of reflecting elements. Here, the computational complexity of the two methods proposed in Subsection IV-A and IV-B will be discussed, and it will show that these methods are computationally acceptable.

Firstly, the complexity of **Algorithm 2** is derived as follows. The complexity for computing (18) is $\mathcal{O}(K^3(N+K))$, which is approximate to $\mathcal{O}(NK^3)$ due to $K \ll N$ in general. The complexity for the sorting procedure is $\mathcal{O}(N \log N)$, which can be ignored. The complexity for determining the feasibility of the solution and the value of (17a) is $\mathcal{O}(NKM + K^2M + K^3) \simeq \mathcal{O}(NKM)$. Thus, assuming for I_{iter} iterations, the computational complexity of **Algorithm 2** is $\mathcal{O}(I_{\text{iter}}(NK^3 + N^2KM)) \simeq \mathcal{O}(I_{\text{iter}}N^2KM)$.

Next, we will consider **Algorithm 3**. The worst-case complexity for solving the SDP optimization \mathcal{P}'_3 with interior-point algorithm is $\mathcal{O}(((N+1)^2 + 1)^{4.5}) \simeq \mathcal{O}(N^9)$ [29]. Compared with this, all others can be ignored. Thus, the computational complexity of **Algorithm 3** is $\mathcal{O}(N^9)$.

From the discussion above, both methods are polynomial computational complexity, compared with the exponential computational complexity of the optimal solution. Furthermore, the computational complexity of **Algorithm 3** is much higher than that of **Algorithm 2**.

Now, the convergence will be analyzed. **Algorithm 3** contains no iteration step, which means the convergence does not need to be discussed here. According to **Algorithm 2**, we define $\mathbf{q}^{(i,j)}$ as the value of \mathbf{q} during the i -th iteration and before the change of $\mathbf{q}_{d_j}^{(i)}$. Due to $g(\mathbf{q}^{(i,j)}) \geq g(\mathbf{q}^{(1,j-1)})$ which is discussed in Subsection IV-A, this method is proved converge.

V. SIMULATION RESULTS

A. Simulation Model

In this section, simulation results will be provided to verify the effect of the proposed algorithm for maximizing energy efficiency in an MU-MISO communication scenario. In our simulation, the signal models and channel models are consistent with the discussion in Section II. In Subsection V-B, the convergence of the algorithm will be shown with different BS transmit power. Then, the performance of the proposed algorithm are tested under a wide range of BS transmit power, which is shown in Section V-C. Finally, the impact of the number of RIS elements on EE will be shown in Subsection V-D.

In this subsection, we will introduce the channel model and simulation parameters. We assume a Rician fading channel that consists of both line-of-sight (LoS) and non-line-of-sight (NLoS) components. Specifically, the channel matrix $\mathbf{F}(\mathbf{G})$ can be expressed as follows:

$$\mathbf{F} = z \left(\sqrt{\frac{\kappa}{\kappa+1}} \mathbf{F}_{\text{LoS}} + \sqrt{\frac{1}{\kappa+1}} \mathbf{F}_{\text{NLoS}} \right), \quad (23)$$

where κ is the Rician factor, z is the path loss related to the distance, \mathbf{F}_{LoS} represents the LoS component of the channel \mathbf{F} , and \mathbf{F}_{NLoS} represents the NLoS component of \mathbf{F} , which follows the distribution $[\mathbf{F}_{\text{NLoS}}]_{k\ell} \sim \text{i.i.d. } \mathcal{CN}(0, 1)$. The LoS component \mathbf{F}_{LoS} admits an SV channel structure, i.e.,

$$\mathbf{F}_{\text{LoS}} = \sqrt{NM} \mathbf{a}_N(\theta, \varphi) \mathbf{a}_M^H(\theta', \varphi'), \quad (24)$$

where $(\theta, \varphi), (\theta', \varphi')$ are the azimuth and elevation angles of the beam in the coordinate system of the RIS and the BS, respectively. The steering vectors $\mathbf{a}_N, N = N_1 \times N_2$ and $\mathbf{a}_M, M = M_1 \times M_2$ are defined as

$$\begin{aligned} \mathbf{a}_N(\theta, \varphi) &= \frac{1}{\sqrt{N}} \left[1, e^{j\pi \sin \theta \sin \varphi / \lambda}, \dots, e^{j\pi(N_1-1) \sin \theta \sin \varphi / \lambda} \right]_{N_1}^T \\ &\quad \otimes \left[1, e^{j\pi \cos \varphi / \lambda}, \dots, e^{j\pi(N_2-1) \cos \varphi / \lambda} \right]_{N_2}^T, \\ \mathbf{a}_M(\theta, \varphi) &= \frac{1}{\sqrt{M}} \left[1, e^{j\pi \sin \theta \sin \varphi / \lambda}, \dots, e^{j\pi(M_1-1) \sin \theta \sin \varphi / \lambda} \right]_{M_1}^T \\ &\quad \otimes \left[1, e^{j\pi \cos \varphi / \lambda}, \dots, e^{j\pi(M_2-1) \cos \varphi / \lambda} \right]_{M_2}^T. \end{aligned} \quad (25)$$

Core simulation parameters are shown in **Table I** [14], [30].

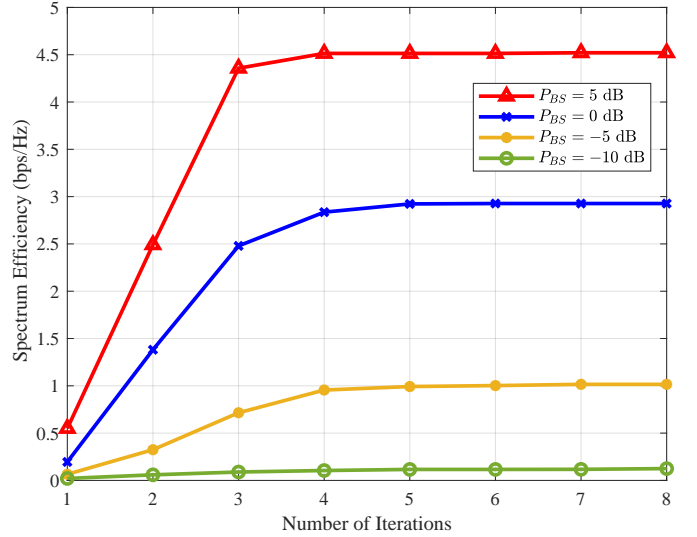


Fig. 2. Convergence performances of the AO algorithm with four different BS transmit power, where the x -axis denotes the number of iterations, y -axis denotes the spectrum efficiency (bps/Hz).

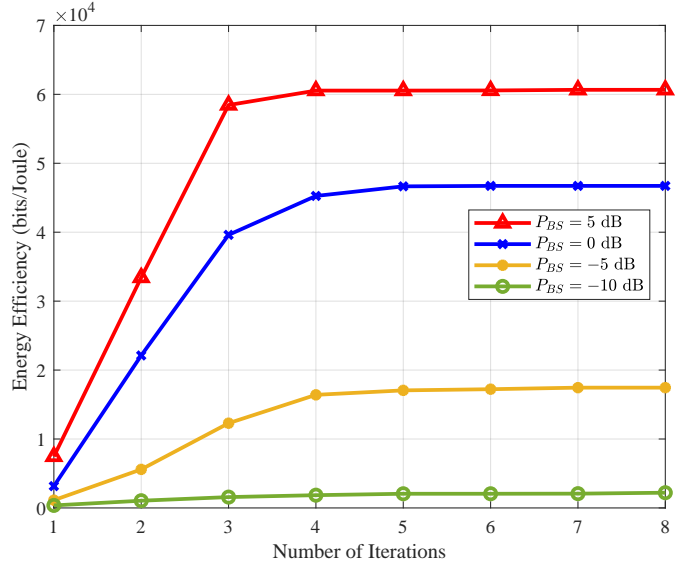


Fig. 3. Convergence performances of the AO algorithm with four different BS transmit power, where the x -axis denotes the number of iterations, y -axis denotes the energy efficiency (bits/Joule).

B. Convergence Performance

In Section III, we have proposed an AO algorithm, which contains 2 steps executed iteratively: Power allocating and RIS analog beamforming. In Subsection III-C, we have theoretically proved the convergence of the algorithm. Here, we will check the convergence rate by numerical simulations. The simulation parameters are shown in **Table I**. The spatial angular coordinates (θ, φ) of BS and user (relative to the RIS) are drawn from a uniform distribution on $[-\pi/2, \pi/2]$ and $M[\pi/3, 2\pi/3]$ respectively.

The SE and EE of the system are studied as a function of the iteration number of the proposed algorithm. Fig. 2 shows the SE of the communication system after each iteration with different BS transmit power, and Fig. 3 shows the evolution of the

TABLE I
SIMULATION PARAMETERS

| | |
|--|------------------------|
| RIS elements $N = N_1 \times N_2$ | $64 = 8 \times 8$ |
| Static power consumption P_{static} | 10 W |
| Power consumption of each ON-state RIS element P_0 | 10 mW |
| Distance between BS and RIS d_{BS} | 200 m |
| Distance between users and RIS d_{UE} | 200 m |
| BS antennas M_{BS} | 8 |
| Number of users K | 4 |
| The minimum SE requirement SE_{min} | 10^{-4} bps/Hz |
| Thermal noise level n_0 | -174 dBm/Hz |
| Carrier frequency f_c | 3.5 GHz |
| Subcarrier spacing BW | 180 kHz |
| Noise power at receiver σ^2 | $\text{BW} \times n_0$ |

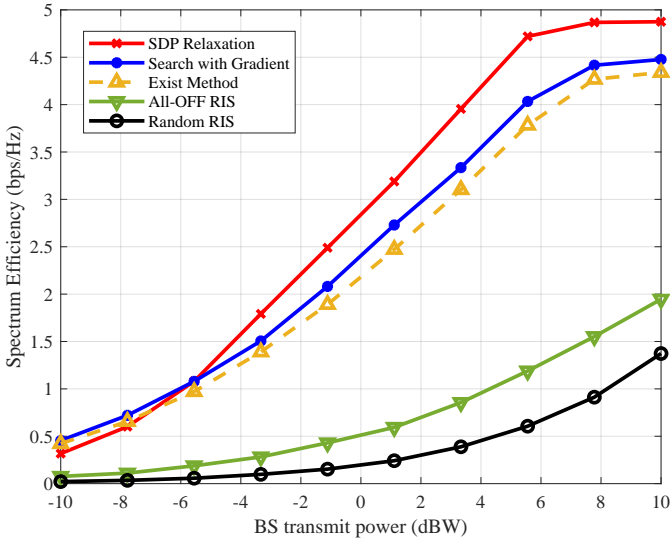


Fig. 4. SE curves based on proposed algorithm, existing method [31], and baselines; x -axis denotes the BS transmit power; y -axis denotes the spectrum efficiency (bps/Hz).

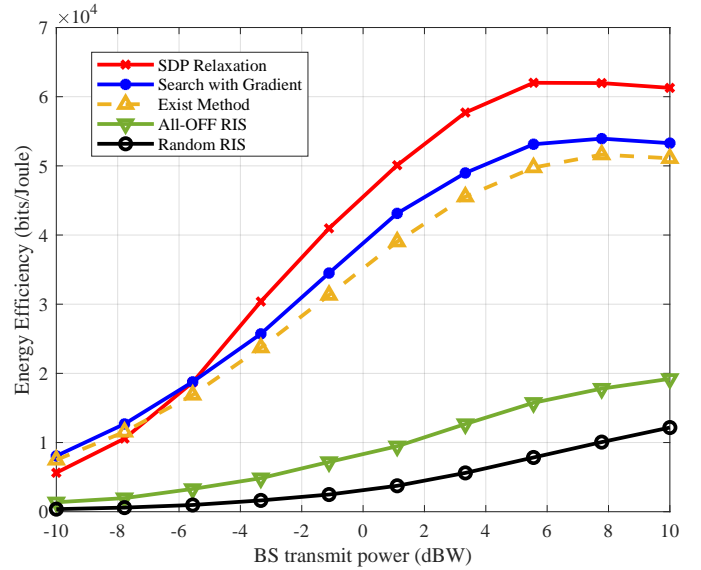


Fig. 5. EE curves based on proposed algorithm, existing method [31], and baselines; x -axis denotes the BS transmit power; y -axis denotes the energy efficiency (bits/Joule).

system EE as the iteration proceeds. These figures show that after several previous iterations, the SE and EE of the system all maintain a stable value, which verifies the convergence of the AO algorithm. Simulation results have demonstrated that, the AO algorithm framework achieves convergence in only two or three iterations. Moreover, this convergence rate is almost independent of the transmitted power, thus proving that the AO algorithm framework is computationally stable and widely applicable to different communication conditions.

C. EE with Different BS Transmit Power

In this subsection, we mainly focus on the energy efficiency optimized by the proposed algorithm as a function of the transmitted power. Note that since the thermal noise power σ_n^2 at the receiver is fixed, the transmitted power admits a constant dB difference from the transmitter signal-to-noise ratio (SNR). The simulation parameters are consistent with those in Subsection V-B, and the BS transmit power varies from -10 dBW to 10 dBW.

The spectrum efficiency and energy efficiency curves are provided in Fig. 4 and Fig. 5. The blue curves “Search with Gradient” in both subgraphs represent the results with the RIS analog beamforming algorithm designed in Subsection IV-A, and the red curves “SDP Relaxation” represent that in Subsection IV-B. It should be noted that both the curves “Search with Gradient” and “SDP Relaxation” belong to the AO framework. Their only difference is that, the former employs the gradient search RIS analog beamforming method, while the latter utilizes the SDP relaxation-based RIS analog beamforming method. The black curves “Random RIS” and the green curves “All-OFF RIS” are baselines, which are given by random RIS analog beamforming and the RIS beamforming as an identity matrix (i.e. all the elements of RIS are configured to the OFF states). We also plot the performance of an existing method proposed in [31], which solves \mathcal{P}_2 via successively setting the phase shifts of all elements in order from $n = 1$ to $n = N$, and update each θ_n by fixing all other θ_k 's, $\forall k \neq n$.

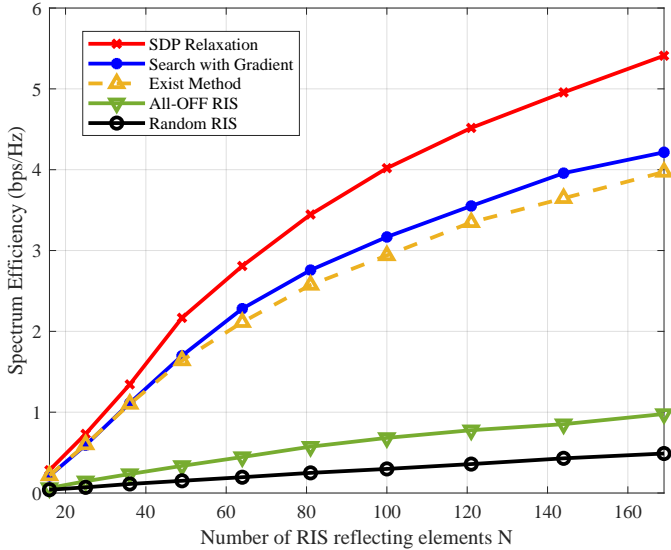


Fig. 6. SE curves based on proposed algorithm, existing method [31], and baselines; x -axis denotes the number of RIS reflecting elements; y -axis denotes the spectrum efficiency (bps/Hz).

The process does not stop until convergence.

Fig. 4 and Fig. 5 show that both two methods have better SE and EE performances in typical scenarios than the two baselines, as well as the existing method. The SDP relaxation method may achieve less performance when the BS transmit power is extremely low, but such scenarios are rare in real-world settings. The reason why “Search with Gradient” outperforms the existing method is that additional information provided by the gradient is fully utilized, thus more decrease in \mathcal{P}_2 's objective function can be achieved in each iteration. There is a noteworthy phenomenon that both the SE and EE curves will reach a platform, where the value will not continuously grow as the increasing BS transmit power. This is because in order to maximize energy efficiency, the power BS consumed to transmit messages is expected low. Thus, even if the potential transmitted power is relatively high, the optimization algorithm tends to transmit with insufficient power, which causes the SE and EE curves flat when BS transmit power restriction is high enough.

We can learn from the figure that the SDP relaxation method proposed in Subsection IV-B is generally better than the gradient searching method proposed in Subsection IV-A. This is reasonable because the solution of optimization problem \mathcal{P}'_2 is provided the approximate value in the real sense only by the latter one, while the former one only provides an effective method for a better solution. However, in Fig. 4, we notice that the results seem to be less significant when BS transmit power is relatively high, which is due to the balance between the increase of SE and the decrease of BS power consumption. In order to get a higher EE, the lower SE carrying by the lower BS power consumption is hard to avoid, and this is particularly prominent under high BS power consumption.

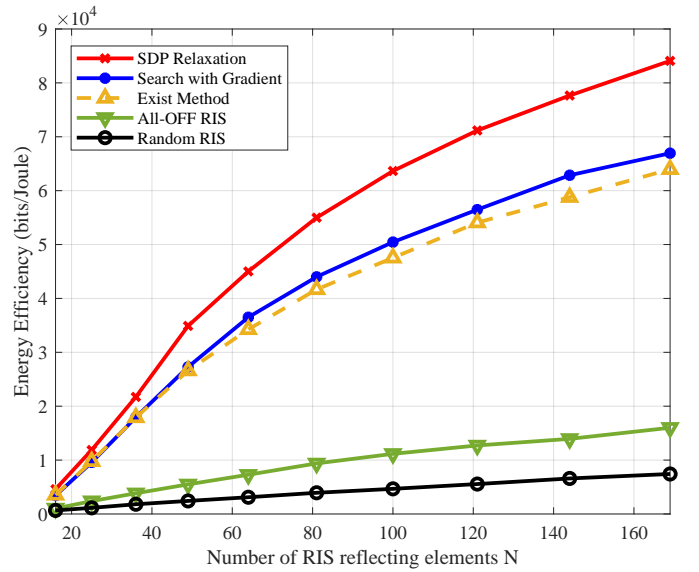


Fig. 7. EE curves based on proposed algorithm, existing method [31], and baselines; x -axis denotes the number of RIS reflecting elements; y -axis denotes the energy efficiency (bits/Joule).

D. Impact of the Number of RIS Elements

Here, we mainly show the impact of the number of RIS reflecting elements on the SE and EE. The simulation parameters are consistent with those in Subsection V-B, and the number of RIS reflecting elements varies from 4×4 to 13×13 .

Fig. 6 and Fig. 7 show the SE and EE curves of the communication system by both two methods. The trends of the five curves are similar to those in Subsection V-C, which represents the performance of algorithms and the baselines respectively. From Fig. 6 and Fig. 7, it is obvious that the SE and EE of the communication system arise as the number of RIS reflecting elements increases, for the stronger beamforming effect by RIS. Also, it shows that the optimization effect of the SDP relaxation method is better than that of the gradient searching method, and both are better than that of baselines, which accords with the above results. This also shows the generality of the proposed algorithm.

VI. CONCLUSION

In this paper, in order to improve the energy efficiency of RIS-assisted MU-MISO systems, we adopted a more accurate power dissipation model for 1-bit RIS elements based on the prevailing PIN-based RIS fabrication technologies. Based on this improved RIS power model, the energy efficiency has been formulated and optimized by jointly minimizing the active transmitted power and the passive RIS power dissipation. The joint optimization problem is first formulated as a non-convex integer programming problem, and then the non-convexity is addressed by rank-1 SDP relaxation. Convergence of the proposed algorithm has been verified by both theoretical analysis and numerical computations. Simulation results have demonstrated that, the energy efficiency of the proposed joint passive-active power minimizing algorithm outperforms that of the existing methods.

For future works, the 1-bit RIS power dissipation model can be generalized to more practical multi-bit versions for improved accuracy. The corresponding joint optimization algorithms can be re-designed to adapt to this enhanced RIS manipulation capability.

APPENDIX A

ANALYTICAL SOLUTION OF THE PROBLEM (14a)

Here, we will analytically solve the optimization problem (14a), which is

$$\mathcal{P}_A : \mathbf{P} = \arg \max_{\mathbf{P}} \sum_{k=1}^K \log_2 \left(1 + \frac{p_k}{\sigma_n^2} \right) - \lambda \left(P_1 + \sum_{k=1}^K p_k t_k \right), \quad (26a)$$

$$\text{s.t.} \quad \sum_{k=1}^K p_k t_k \leq P_{\max}, \quad (26b)$$

$$p_k \geq p_{\min}, \quad \forall k \in \mathcal{K}. \quad (26c)$$

As shown above, the target is to maximize a concave function (26a) with affine constraints (26b) and (26c). Firstly, the Lagrange function of \mathcal{P}_A can be expressed as

$$\begin{aligned} \mathcal{L}(p_k, \boldsymbol{\mu}) &= \lambda \left(P_1 + \sum_{k=1}^K p_k t_k \right) - \sum_{k=1}^K \log_2 \left(1 + \frac{p_k}{\sigma_n^2} \right) \\ &\quad + \mu_0 \left(\sum_{k=1}^K p_k t_k - P_{\max} \right) - \sum_{k=1}^K \mu_k (p_k - p_{\min}). \end{aligned} \quad (27)$$

Then, the KKT condition of \mathcal{P}_A can be written as

$$(\lambda + \mu_0) t_k - \mu_k - \frac{1}{(p_k + \sigma_n^2) \log 2} = 0, \quad \forall k \in \mathcal{K}, \quad (28a)$$

$$\mu_0 \left(\sum_{k=1}^K p_k t_k - P_{\max} \right) = 0, \quad (28b)$$

$$\mu_k (p_k - p_{\min}) = 0, \quad \forall k \in \mathcal{K}, \quad (28c)$$

$$\mu_0, \mu_k \geq 0, \quad \forall k \in \mathcal{K}. \quad (28d)$$

These are similar to water-filling solutions in form, but the relaxation term with λ makes some difference. Here, we substitute (28c) into (28a), and then we obtain

$$p_k = \max \left\{ \frac{1}{\log 2} \frac{1}{(\lambda + \mu_0) t_k} - \sigma_n^2, p_{\min} \right\}. \quad (29)$$

With the equation (28b), we have

$$\mu_0 \left(\sum_{k=1}^K \max \left\{ \frac{1}{\log 2} \frac{1}{\lambda + \mu_0} - t_k \sigma_n^2, p_{\min} t_k \right\} - P_{\max} \right) = 0. \quad (30)$$

Then, after introducing two auxiliary variables, the analytical solution of \mathcal{P}_A can be written as

$$\zeta : \sum_{k=1}^K \max \left\{ \zeta - t_k \sigma_n^2, t_k p_{\min} \right\} = P_{\max}, \quad (31a)$$

$$\xi = \min \left\{ \zeta, \frac{1}{\lambda \log 2} \right\}, \quad (31b)$$

$$p_k = \max \left\{ \frac{1}{t_k} (\xi - t_k \sigma_n^2), p_{\min} \right\}. \quad (31c)$$

APPENDIX B

PROOF OF THE EQUIVALENCE BETWEEN \mathcal{P}'_2 AND \mathcal{P}_3

In order to simplify the problem, we define the variable matrix \mathbf{X} in order to replace \mathbf{q} , which can be expressed as

$$\mathbf{X} = \begin{bmatrix} \mathbf{q} \\ 1 \end{bmatrix} \begin{bmatrix} \mathbf{q}^T & 1 \end{bmatrix} = \begin{bmatrix} \mathbf{q}\mathbf{q}^T & \mathbf{q} \\ \mathbf{q}^T & 1 \end{bmatrix}, \quad (32)$$

where $\mathbf{q}\mathbf{q}^T$ can replace the quadratic term, and \mathbf{q} or \mathbf{q}^T can replace the linear term. The expression of $\mathbf{H}^H \mathbf{H}$ can be derived as follows

$$\begin{aligned} \mathbf{H}^H \mathbf{H} &= \mathbf{F}^H \boldsymbol{\Theta} \mathbf{G} \mathbf{G}^H \boldsymbol{\Theta} \mathbf{F} \\ &= \mathbf{F}^H \text{diag}(\mathbf{q}) \mathbf{G} \mathbf{G}^H \text{diag}(\mathbf{q}) \mathbf{F}. \end{aligned} \quad (33)$$

Then, we consider the (i, j) -element of matrix $\text{diag}(\mathbf{q}) \mathbf{G} \mathbf{G}^H \text{diag}(\mathbf{q})$, which is

$$\begin{aligned} &[\text{diag}(\mathbf{q}) \mathbf{G} \mathbf{G}^H \text{diag}(\mathbf{q})]_{(i,j)} \\ &= \sum_{k=1}^N \sum_{l=1}^N [\text{diag}(\mathbf{q})]_{(i,k)} [\mathbf{G} \mathbf{G}^H]_{(k,l)} [\text{diag}(\mathbf{q})]_{(l,j)} \\ &= \sum_{k=1}^N \sum_{l=1}^N q_i q_j [\mathbf{G} \mathbf{G}^H]_{(k,l)} \delta_{ik} \delta_{lj} \\ &= q_i q_j [\mathbf{G} \mathbf{G}^H]_{(i,j)}, \end{aligned} \quad (34)$$

so the matrix above can be expressed as the Hadamard product $\mathbf{q}\mathbf{q}^T \odot \mathbf{G} \mathbf{G}^H$, which can be written as a linear combination of \mathbf{X} . Then, the matrix $\mathbf{H}^H \mathbf{H}$ can be expressed as

$$\mathbf{H}^H \mathbf{H} = \mathbf{F}_0^H (\mathbf{X} \odot \mathbf{G}_0) \mathbf{F}_0, \quad (35)$$

where the \mathbf{F}_0 and \mathbf{G}_0 are defined in (21). Then, the constraint (17b) can be written as

$$\begin{aligned} &\text{tr} \left(\mathbf{P}^{\frac{1}{2}} (\mathbf{H}^H \mathbf{H})^{-1} \mathbf{P}^{\frac{1}{2}} \right) \\ &= \text{tr} \left((\mathbf{F}_0^H (\mathbf{X} \odot \mathbf{G}_0) \mathbf{F}_0 \mathbf{P}^{-1})^{-1} \right) \leq P_{\max}. \end{aligned} \quad (36)$$

The other constraint (17c) of \mathcal{P}'_2 can also be written as

$$q_n^2 = 1, \quad \forall n \in \mathcal{N}, \quad (37)$$

which means the diagonal of \mathbf{X} (i.e. q_n^2) is always 1, which leads to $N + 1$ constraints

$$\text{tr}(\mathbf{E}_{i,i} \mathbf{X}) = 1. \quad (38)$$

In addition, according to (32), the semi-definite constraint $\mathbf{X} \succeq 0$ and the rank-one constraint $\text{rank}(\mathbf{X}) = 1$ should be considered in order to ensure the equivalence. This completes the proof.

REFERENCES

- [1] Z. Li, J. Zhang, J. Zhu, and L. Dai, "RIS energy efficiency optimization with practical power models," in *Proc. 2023 IEEE Int. Wireless Commun. and Mobile Comput. Conf. (IWCMC)*, Jun. 2023, pp. 1172–1177.
- [2] M. Di Renzo, A. Zappone, M. Debbah, M.-S. Alouini, C. Yuen, J. De Rosny, and S. Tretyakov, "Smart radio environments empowered by reconfigurable intelligent surfaces: How it works, state of research, and the road ahead," *IEEE J. Sel. Areas Commun.*, vol. 38, no. 11, pp. 2450–2525, Nov. 2020.

- [3] C. Pan, H. Ren, K. Wang, J. F. Kolb, M. El-kashlan, M. Chen, M. Di Renzo, Y. Hao, J. Wang, A. L. Swindlehurst, X. You, and L. Hanzo, "Reconfigurable intelligent surfaces for 6G systems: Principles, applications, and research directions," *IEEE Commun. Mag.*, vol. 59, no. 6, pp. 14–20, Jun. 2021.
- [4] Q. Wu and R. Zhang, "Towards smart and reconfigurable environment: Intelligent reflecting surface aided wireless network," *IEEE Commun. Mag.*, vol. 58, no. 1, pp. 106–112, Jan. 2020.
- [5] K. Liu, Z. Zhang, L. Dai, and L. Hanzo, "Compact user-specific reconfigurable intelligent surface for uplink transmission," *IEEE Trans. Commun.*, vol. 70, no. 1, pp. 680–692, Jan. 2021.
- [6] E. Basar, M. Di Renzo, J. De Rosny, M. Debbah, M.-S. Alouini, and R. Zhang, "Wireless communications through reconfigurable intelligent surfaces," *IEEE Access*, vol. 7, pp. 116753–116773, Aug. 2019.
- [7] Q. Wu and R. Zhang, "Intelligent reflecting surface enhanced wireless network via joint active and passive beamforming," *IEEE Trans. Wireless Commun.*, vol. 18, no. 11, pp. 5394–5409, Nov. 2019.
- [8] Q. Wu, G. Y. Li, W. Chen, D. W. K. Ng, and R. Schober, "An overview of sustainable green 5G networks," *IEEE Wireless Commun.*, vol. 24, no. 4, pp. 72–80, Aug. 2017.
- [9] J.-B. Gros, V. Popov, M. A. Odit, V. Lenets, and G. Lerosey, "A reconfigurable intelligent surface at mmwave based on a binary phase tunable metasurface," *IEEE Open J. Commun. Society*, vol. 2, pp. 1055–1064, May 2021.
- [10] M. Cui, Z. Wu, Y. Chen, S. Xu, F. Yang, and L. Dai, "Demo: Low-power communications based on RIS and AI for 6G," in *Proc. IEEE Int. Conf. Commun. (IEEE ICC'22, Demo Session)*, May 2022.
- [11] A. Araghi, M. Khalily, M. Safaei, A. Bagheri, V. Singh, F. Wang, and R. Tafazolli, "Reconfigurable intelligent surface (RIS) in the sub-6 GHz band: Design, implementation, and real-world demonstration," *IEEE Access*, vol. 10, pp. 2646–2655, Jan. 2022.
- [12] F. Zhang, Q. Zhao, W. Zhang, J. Sun, J. Zhou, and D. Lippens, "Voltage tunable short wire-pair type of metamaterial infiltrated by nematic liquid crystal," *Appl. Phys. Lett.*, vol. 97, no. 13, pp. 103–134, Sep. 2010.
- [13] M. Ismail, M. Rahim, and H. Majid, "The investigation of PIN diode switch on reconfigurable antenna," in *Proc. 2011 IEEE Int. RF & Microw. Conf.*, Dec. 2011, pp. 234–237.
- [14] J. Wang, W. Tang, J. C. Liang, L. Zhang, J. Y. Dai, X. Li, S. Jin, Q. Cheng, and T. J. Cui, "Reconfigurable intelligent surface: Power consumption modeling and practical measurement validation," *arXiv preprint arXiv:2211.00323*, Nov. 2022.
- [15] C. Huang, G. C. Alexandropoulos, A. Zappone, M. Debbah, and C. Yuen, "Energy efficient multi-user MISO communication using low resolution large intelligent surfaces," in *Proc. 2018 IEEE Globecom Workshops (GC Wkshps)*, 2018, pp. 1–6.
- [16] R. Méndez-Rial, C. Rusu, N. González-Prelcic, A. Alkhateeb, and R. W. Heath, "Hybrid MIMO architectures for millimeter wave communications: Phase shifters or switches?" *IEEE Access*, vol. 4, pp. 247–267, 2016.
- [17] C. Huang, A. Zappone, G. C. Alexandropoulos, M. Debbah, and C. Yuen, "Reconfigurable intelligent surfaces for energy efficiency in wireless communication," *IEEE Trans. Wireless Commun.*, vol. 18, no. 8, pp. 4157–4170, Aug. 2019.
- [18] S. P. Boyd and L. Vandenberghe, *Convex optimization*. Cambridge, U.K.: Cambridge University Press, 2004.
- [19] J. Yuan, Y.-C. Liang, J. Joung, G. Feng, and E. G. Larsson, "Intelligent reflecting surface-assisted cognitive radio system," *IEEE Trans. Commun.*, vol. 69, no. 1, pp. 675–687, Jan. 2021.
- [20] Q. Wu, G. Y. Li, W. Chen, D. W. K. Ng, and R. Schober, "An overview of sustainable green 5G networks," *IEEE Wireless Commun.*, vol. 24, no. 4, pp. 72–80, Aug. 2017.
- [21] R. Mahapatra, Y. Nijsure, G. Kaddoum, N. Ul Hassan, and C. Yuen, "Energy efficiency tradeoff mechanism towards wireless green communication: A survey," *IEEE Commun. Surv. Tutor.*, vol. 18, no. 1, pp. 686–705, Oct. 2016.
- [22] L. You, J. Xiong, D. W. K. Ng, C. Yuen, W. Wang, and X. Gao, "Energy efficiency and spectral efficiency tradeoff in RIS-aided multiuser MIMO uplink transmission," *IEEE Trans. Signal Process.*, vol. 69, pp. 1407–1421, Dec. 2021.
- [23] V. Arun and H. Balakrishnan, "RFocus: Beamforming using thousands of passive antennas," in *Proc. 17th USENIX Symp. Netw. Syst. Design and Implement. (NSDI'20)*, Feb. 2020.
- [24] X. Pei, H. Yin, L. Tan, L. Cao, Z. Li, K. Wang, K. Zhang, and E. Björnson, "RIS-aided wireless communications: Prototyping, adaptive beamforming, and indoor/outdoor field trials," *IEEE Trans. Commun.*, vol. 69, no. 12, pp. 8627–8640, Dec. 2021.
- [25] C.-K. Wen, S. Jin, and K.-K. Wong, "On the sum-rate of multiuser MIMO uplink channels with jointly-correlated rician fading," *IEEE Trans. Commun.*, vol. 59, no. 10, pp. 2883–2895, Oct. 2011.
- [26] C. Peel, B. Hochwald, and A. Swindlehurst, "A vector-perturbation technique for near-capacity multiantenna multiuser communication-part I: channel inversion and regularization," *IEEE Trans. Commun.*, vol. 53, no. 1, pp. 195–202, Jan. 2005.
- [27] A. M.-C. So, J. Zhang, and Y. Ye, "On approximating complex quadratic optimization problems via semidefinite programming relaxations," *Math. Program.*, vol. 110, no. 1, pp. 93–110, Jun. 2007.
- [28] M. Grant and S. Boyd, "CVX: Matlab software for disciplined convex programming, version 2.1," <http://cvxr.com/cvx>, Mar. 2014.
- [29] Z. Luo, W. Ma, A. M. So, Y. Ye, and S. Zhang, "Semidefinite relaxation of quadratic optimization problems," *IEEE Signal Process. Mag.*, vol. 27, no. 3, pp. 20–34, Mar. 2010.
- [30] J. Zhu, K. Liu, Z. Wan, L. Dai, T. J. Cui, and H. V. Poor, "Sensing RISs: Enabling dimension-independent CSI acquisition for beamforming," *IEEE Trans. Inf. Theory*, vol. 22, no. 5, pp. 3795–3813, Jun. 2023.
- [31] Q. Wu and R. Zhang, "Beamforming optimization for wireless network aided by intelligent reflecting surface with discrete phase shifts," *IEEE Trans. Commun.*, vol. 68, no. 3, pp. 1838–1851, Mar. 2020.